The 8th European Congress on Computational Methods in Applied Sciences and Engineering
ECCOMAS Congress 2022
5-–9 June 2022, Oslo, Norway

ENERGY-PRESERVING STABLE COMPUTATIONS OF HIGH-PRESSURE SUPERCRITICAL FLUIDS TURBULENCE

Marc Bernades[1], Francesco Capuano[1], F. Xavier Trias[2] and Lluís Jofre[1]

[1] Dept. Fluid Mechanics, Technical University of Catalonia, Barcelona 08019, Spain

[2] Heat and Mass Transfer Technological Center, Technical University of Catalonia, C/Colom 11, 08222 Terrassa (Barcelona), Spain

Key words: Energy-preserving schemes, High-pressure, Supercritical fluids, Turbulence

Abstract. High-fidelity computations of turbulent flows at high-pressure supercritical fluid conditions present significant challenges. Besides the inherent broadband nature of the flow, the rapid variation of thermophysical properties across the pseudo-boiling region can result in additional complexities in terms of strong localized density gradients, spurious pressure oscillations, non-linear behaviour of fluids, and amplification of aliasing errors. Different research groups have utilized distinct approaches to achieve numerical stability, mostly resorting to upwind-biased schemes, artificial dissipation and/or high-order filtering. However, in these strategies, stability is achieved at the expense of artificially suppressing part of the turbulent energy spectrum. In this regard, this work aims to explore the suitability, in terms of stability and accuracy, of recently proposed energy-preserving schemes for scale-resolving simulations of supercritical turbulence. For ideal gases, such type of methods have been demonstrated to provide stable and accurate computations of turbulence by preserving kinetic energy and/or other quantities of physical relevance. However, their extension to real-gas thermodynamic frameworks is still in its infancy, and consequently requires to be carefully investigated. To this objective, this work analyzes the performance of different classical and energy-preserving discretizations under ideal-gas conditions, and carries out an initial assessment of their performance at high-pressure supercritical fluid regimes. The results obtained indicate that their extension to real-gas thermodynamics is not straightforward, and consequently motivate the necessity to develop new solutions able to satisfy the desired stability and accuracy requirements.

1 INTRODUCTION

Supercritical fluids operate within high-pressure thermodynamic spaces in which intermolecular forces and finite packing volume effects become important. In this regard, it is important to distinguish between supercritical gas-like and liquid-like fluids [1, 2]: (i) a supercritical liquid-like fluid is one whose density is large, and whose transport coefficients behave similar to a liquid; (ii) the density of supercritical gas-like fluids is smaller, and their transport coefficients vary similar to gases. This set of thermophysical characteristics presents very interesting properties that can be leveraged to achieve turbulent regimes in microfluidic devices [3], which is, for example, very

important for microscale energy applications since turbulence is a very efficient flow mechanism for enhancing mixing and transfer rates [4].

The non-linearity of real-gas thermodynamics, however, imposes significantly complex challenges, mainly in terms of numerical stability, to the discretization schemes utilized for computationally studying the turbulent flow motion of supercritical fluids. In particular, the rapid (smooth) variations of density, viscosity and thermal conductivity across the pseudo-boiling region result in spurious pressure oscillations that can contaminate the numerical solution and even lead to a blow-up of the computations. This is further complicated by the multiscale nature of turbulence, which necessitates dedicated numerical schemes that are simultaneously: i) exempt of artificial dissipation, to properly capture the significantly wide range of spatio-temporal flow scales, and ii) non-linearly stable, to prevent unbounded amplification of aliasing errors. Therefore, the numerical solution of supercritical fluids turbulence ultimately requires methods that are (i) able to represent the wide range of turbulent scales (non-dissipative), ii) non-linearly stable, (iii) free of artificial pressure oscillations, and (iv) computationally fast (efficient).

Standard numerical approaches employed for solving the compressible equations of fluid motion have been historically based on discretizing the conservative (*divergence*) formulation of the Navier-Stokes equations, in conjunction with stabilizing methods that can be categorized in two main groups: (i) filtering [5, 6, 7] based on high-order filters applied to the conserved variables to achieve stability and robustness, however, at expenses of suppressing part of the turbulent scales; and (ii) upwind-biased methods developed mostly for capturing shocks, such as HLLC [8] and WENO schemes [9], which are known to add exceedingly high levels of artificial dissipation into the numerical solutions. On the other hand, kinetic-energy preserving schemes based on *split* forms of the convective term, like the one proposed by Kennedy & Gruber [10] and later shown to be energy-preserving by Pirozzoli [11] — referred to as KGP hereinafter —, are becoming a popular choice for solving compressible turbulence [12]. These methods have been shown to be stable and non-dissipative for a wide range of ideal-gas flow configurations at high Reynolds numbers [13], but they are yet to be assessed for supercritical fluids turbulence.

Real-gas thermodynamic modeling frameworks come with additional challenges. Classical numerical schemes are unable to maintain pressure equilibrium with constant velocity and pressure, a fact which is true even for ideal-gas models [14]. This is further exacerbated by the non-linear thermodynamics of real gases, leading to the well-known problem of pressure oscillations [15, 16, 17]. Some specific strategies that have been developed to deal with the above issues include: (i) double-flux scheme [18] based on the concept of "frozen thermodynamics", which fixes the internal energy within the time-integration step to artificially enforce pressure equilibrium, at the expenses of modifying the thermodynamics; (ii) pressure-based approaches [19, 15] that evolve the pressure equation, rather than e.g., the total energy, to prevent pressure oscillations; (iii) Lacaze et al. [17] proposed a hybrid methodology evolving pressure and energy without proper conservation of enthalpy; and (iv) filters, similar to the strategies described for ideal gases above, which is an undesirable solution due to its inherent loss of accuracy.

The objectives of this work are twofold: (i) assess the performances, in terms of energy conservation and pressure oscillations, of several state-of-the-art methods under ideal-gas conditions, and (ii) explore the extension of energy-preserving schemes to high-pressure supercritical fluid regimes. First, in Section 2, the flow physics modeling of supercritical fluids is presented. Next, the discretization frameworks considered in this work are described and numerically analyzed in

Section 3. Furthermore, the numerical results are presented in Section 4. Finally, in Section 5, the work is concluded, and future directions are proposed.

2 FLOW PHYSICS MODELING

The flow physics modeling of supercritical fluids turbulence in terms of (i) equations of fluid motion and (ii) real-gas thermodynamics is described in the subsections below.

2.1 Equations of fluid motion

The turbulent flow motion of supercritical fluids is described by the following set of conservation equations of mass, momentum, and total energy

$$\frac{\partial \rho}{\partial t} + \nabla \cdot (\rho \mathbf{v}) = 0, \tag{1}$$

$$\frac{\partial (\rho \mathbf{v})}{\partial t} + \nabla \cdot (\rho \mathbf{v}\mathbf{v}) = -\nabla P + \nabla \cdot \boldsymbol{\tau}, \tag{2}$$

$$\frac{\partial (\rho E)}{\partial t} + \nabla \cdot (\rho \mathbf{v} E) = -\nabla \cdot \boldsymbol{q} - \nabla \cdot (P\mathbf{v}) + \nabla \cdot (\boldsymbol{\tau} \cdot \mathbf{v}), \tag{3}$$

where ρ is the density, $\mathbf{v}$ is the velocity vector, P is the pressure, $\boldsymbol{\tau}$ is the viscous stress tensor for Newtonian fluids, E is the total energy, and $\boldsymbol{q}$ is the Fourier conduction heat flux.

2.2 Real-gas thermodynamics

The thermodynamic space of solutions for the state variables pressure P, temperature T, and density ρ of a single substance is described by an equation of state. One popular choice for systems at high pressures, which is used in this study, is the Peng-Robinson equation of state [20] written as

$$P = \frac{R_u T}{\bar{v} - b} - \frac{a}{\bar{v}^2 + 2b\bar{v} - b^2}, \tag{4}$$

with R_u the universal gas constant, $\bar{v} = W/\rho$ the molar volume, and W the molecular weight. The coefficients a and b take into account real-gas effects related to attractive forces and finite packing volume, respectively, and depend on the critical temperatures T_c, critical pressures P_c, and acentric factors ω. They are defined as

$$a = 0.457 \frac{(\mathrm{R_u} T_c)^2}{P_c} \left[1 + c\left(1 - \sqrt{T/T_c}\right)\right]^2 \quad \text{and} \quad b = 0.078 \frac{\mathrm{R_u} T_c}{P_c}, \tag{5}$$

where coefficient c is provided by

$$c = \begin{cases} 0.380 + 1.485\omega - 0.164\omega^2 + 0.017\omega^3 & \text{if } \omega > 0.49, \\ 0.375 + 1.542\omega - 0.270\omega^2 & \text{otherwise.} \end{cases} \tag{6}$$

The Peng-Robinson real-gas equation of state needs to be supplemented with the corresponding high-pressure thermodynamic variables based on departure functions [21] calculated as a difference between two states. In particular, their usefulness is to transform thermodynamic variables from ideal-gas conditions (low pressure - only temperature dependant) to supercritical

conditions (high pressure). The ideal-gas parts are calculated by means of the NASA 7-coefficient polynomial [22], while the analytical departure expressions to high pressures are derived from the Peng-Robinson equation of state as detailed in Jofre & Urzay [2].

3 DISCRETIZATION FRAMEWORKS

3.1 Energy-preserving schemes

In this framework, the equations of fluid motion introduced in Section 2.1 are numerically tackled by adopting a standard semi-discretization procedure, i.e., they are firstly discretized in space and then integrated in time. Spatial differential operators are treated using centered finite-differencing formulas; a second-order centered scheme is used in this paper, although the results can be easily generalized to formulas of any order that satisfy a discrete summation-by-parts rule. The temporal errors that arise due to the time-integration scheme (in this case a Runge-Kutta method) are assumed to be kept under control by using sufficiently small time steps [23].

The convective terms of Eqs. (1)-(3) can be rewritten with a common structure

$$C = \frac{\partial \rho u_j \phi}{\partial x_j}, \tag{7}$$

where ϕ is the transported scalar. The derivation of kinetic-energy-preserving (KEP) methods relies on the preliminary observation that the general convective term in Eq. (7) can be equivalently expressed as follows, using the product rule [12]

$$C^D = \frac{\partial \rho u_j \phi}{\partial x_j}, \tag{8}$$

$$C^\phi = \phi \frac{\partial \rho u_j}{\partial x_j} + \rho u_j \frac{\partial \phi}{\partial x_j}, \tag{9}$$

$$C^u = u_j \frac{\partial \rho \phi}{\partial x_j} + \rho \phi \frac{\partial u_j}{\partial x_j}, \tag{10}$$

$$C^\rho = \rho \frac{\partial u_j \phi}{\partial x_j} + \phi u_j \frac{\partial \rho}{\partial x_j}, \tag{11}$$

$$C^L = \rho \phi \frac{\partial u_j}{\partial x_j} + \rho u_j \frac{\partial \phi}{\partial x_j} + \phi u_j \frac{\partial \rho}{\partial x_j}. \tag{12}$$

Equation (8) is the usual divergence (conservative) form, whereas linear combination of Eqs. (8)-(12) are consistent expressions of the nonlinear convective term. However, the corresponding discretization behave differently due to product rule, which does not hold for discrete operators. These differences clearly emerge when considering induced quantities such as kinetic energy. In this regard, convective terms for mass and generic variable ϕ can be expressed as

$$\mathcal{M} = \xi \mathcal{M}^D + (1 - \xi)\mathcal{M}^A, \tag{13}$$

$$C = \alpha C^D + \beta C^\phi + \gamma C^u + \delta C^\rho + \epsilon C^L, \tag{14}$$

where ξ is an arbitrary coefficient and $\alpha + \beta + \gamma + \delta + \epsilon = 1$, and $\mathcal{M}^D$ and $\mathcal{M}^A$ are divergence and advective forms in continuity equation.

To ensure that the nonlinear terms do not spuriously contribute to the global kinetic energy balance, the satisfying condition leads to following constraints, with a two-parameter family of possible energy-preserving formulations [12, 10]

$$\begin{cases} \alpha & = 1/2 - \delta, \\ \beta & = \xi/2, \\ \gamma & = \delta, \\ \epsilon & = \frac{1-\xi}{2} - \delta. \end{cases} \tag{15}$$

Here the attention will be focused on the so-called KGP split form, which is obtained by setting $\epsilon = 0$ (sufficient condition for local conservation) and $\beta = \gamma = \delta = 1/4$ [10, 11]. When applied to the continuity and momentum equations, the KGP scheme globally preserves kinetic energy by convection and locally and globally preserves mass and momentum. In terms of the energy equation, total energy is evolved and the KGP splitting is applied to the enthalpy $h = e + P/\rho$. This choice leads to conservation of internal energy, and has proved to be particularly robust in previous works [12]. Alternative formulations (both in terms of the split formulation and the energy equation) are not studied here and are left for future work.

3.2 Pressure-equilibrium-preserving schemes

Another topic that has received considerable attention is the pressure-equilibrium-preserving (PEP) property of numerical schemes. Under ideal gas conditions, i.e., $\rho e = P/(\gamma - 1)$, the pressure-evolution equation can be easily obtained from the internal energy equation, and reads (here shown for a 1D inviscid case)

$$\frac{\partial P}{\partial t} = -\frac{\partial Pu}{\partial x} - (\gamma - 1)P\frac{\partial u}{\partial x}. \tag{16}$$

Additionally, the one-dimensional velocity-evolution equation can be derived by subtracting the mass equation multiplied by velocity from the momentum equation, yielding

$$\frac{\partial u}{\partial t} = -\frac{1}{\rho}(\frac{\partial \rho uu}{\partial x} + \frac{\partial P}{\partial x} - u\frac{\partial \rho u}{\partial x}). \tag{17}$$

Based on Eqs. (16)-(17), it can be deduced that when the initial pressure and velocity are spatially constant (with density varying in space), then neither pressure nor velocity change in time; it is therefore highly desirable that this equilibrium is discretely preserved in numerical simulations, leading to the concept of PEP schemes.

In the case of KEP schemes, the discrete total energy equation can be considered as the sum of kinetic and internal energy equation, and thus the semi-discrete internal energy equation is

$$\frac{\partial \rho e}{\partial t} + \frac{\widetilde{\mathcal{I}}|_{(m+1/2)} - \widetilde{\mathcal{I}}|_{(m-1/2)}}{\Delta x} + P\frac{u|_{(m+1)} - u|_{(m-1)}}{2\Delta x}, \tag{18}$$

where $\widetilde{\mathcal{I}}$ is the internal energy flux and m denotes the cell index. In the KEP approach described in Section 3.1, the internal energy flux can be expressed as follows

$$\widetilde{\mathcal{I}}|_{(m\pm1/2)} = \frac{\rho|_{(m\pm1)} + \rho|_{(m)}}{2}\frac{e|_{(m\pm1)} + e|_{(m)}}{2}\frac{u_j|_{(m\pm1)} + u_j|_{(m)}}{2}. \tag{19}$$

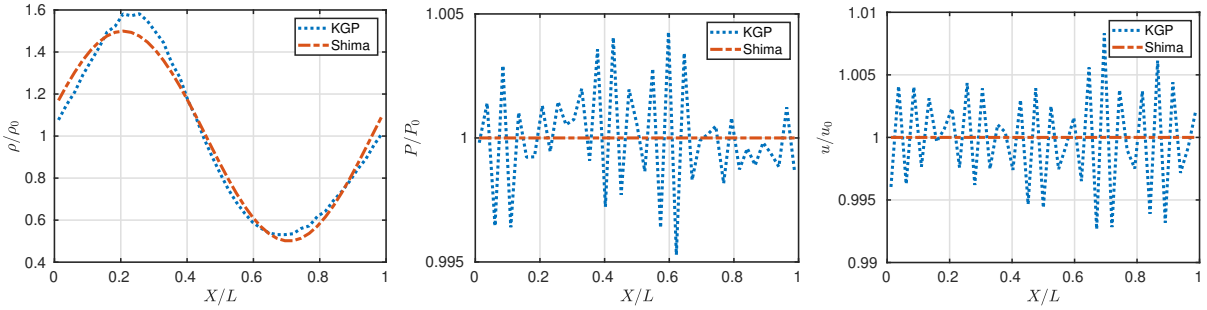

(a) (b) (c)

Figure 1: 1D Advection test with $P_0 = 1\,\mathrm{Pa}$, $u_0 = 1\,\mathrm{m/s}$ and $\rho_0 = 2\,\mathrm{kg/m^3}$ on a domain of length $L = 1$, comparing KGP (dotted line) and Shima et al. (dashed line) convective schemes. Results after 11 cycles for normalized (a) density, (b) pressure and (c) velocity.

Hence, by substituting Eq. (19) and the ideal-gas relation into the discrete internal-energy equation, Eq.(18), the discrete counterpart of Eq. (16) can be obtained, and reads

$$\begin{aligned}\frac{\partial P}{\partial t}|_{(m)} =& \frac{\left[\rho|_{(m+1)} + \rho|_{(m)}\right]\left[u|_{(m+1)} + u|_{(m)}\right]\left[(P/\rho)|_{(m+1)} + (P/\rho)|_{(m)}\right]}{2\Delta x} \\ &- \frac{\left[\rho|_{(m-1)} + \rho|_{(m)}\right]\left[u|_{(m-1)} + u|_{(m)}\right]\left[(P/\rho)|_{(m-1)} + (P/\rho)|_{(m)}\right]}{2\Delta x} \\ &-(\gamma-1)P|_{(m)}\frac{\left[u|_{(m+1)} + u|_{(m-1)}\right]}{2\Delta x}.\end{aligned} \tag{20}$$

Assuming that the initial pressure and velocity are spatially constant and density varies in space, Eq. (20) indicates that the physical pressure equilibrium cannot be numerically guaranteed, as $\partial P/\partial t|_{(m)} \neq 0$. Recently, Shima et al. [14] proposed a flux formulation for the internal energy (while keeping, e.g., KGP split for momentum) able to ensure that $\partial P/\partial t|_{(m)} = 0$:

$$\widetilde{\mathcal{I}}|_{(m\pm1/2)} = \frac{\rho e|_{(m\pm1)} + \rho e|_{(m)}}{2}\frac{u_j|_{(m\pm1)} + u_j|_{(m)}}{2} = \frac{P|_{(m\pm1)} + P|_{(m)}}{2(\gamma-1)}\frac{u_j|_{(m\pm1)} + u_j|_{(m)}}{2}. \tag{21}$$

Numerical results reported in Figure 1 highlight the difference between KGP and PEP (Shima et al.) schemes in terms of preventing pressure oscillations for a 1D advective inviscid test with constant velocity and pressure under ideal gas conditions.

The appearance of pressure oscillations under real-gas frameworks is further exacerbated by the complexities of the thermodynamic model and has been a cause of concern and investigation over the last decade [15, 16, 17]. The extension of the approach reported above for real-gas frameworks becomes particularly involved due to the inherent non-linearity of the model and is not shown here. To the authors' knowledge, there is currently no PEP formulation available for real-gas thermodynamics and high-pressure supercritical conditions.

3.3 Other methods

This sections covers other standard numerical approaches employed for solving the equations of fluid motion for compressible flow considered and tested in this study.

Within the filtering class, many types of approaches can be found in literature; most commonly, high-order implicit filters [5] or Gaussian filters [6] are applied to the conserved variables at each time step. These filters introduce numerical dissipation but are generally successful in stabilizing the solution (when a non-linearly *unstable* scheme is used). For comparison purposes, this work will focus on the second-order Gaussian filter (viz. representative of general symmetric convolution filters) [24]:

$$\bar{\varphi} = \varphi + \frac{\bar{\triangle}^2}{24}\frac{\partial^2 \varphi}{\partial x_i^2} + \mathcal{O}(\bar{\triangle}^4), \tag{22}$$

where $\bar{\varphi}$ is the filtered variable and $\bar{\triangle}$ the filter width (i.e., mesh size). Even though higher-order (possibly implicit) filters are obviously less dissipative, here the stencil is limited to a two-point function for efficiency purposes; indeed, increasing the stencil width is known to significantly deteriorate the parallel performances, especially when dealing with implicit spatial schemes [25].

Alternatively, upwind-biased methods (typically developed for capturing shocks), have been often used to stabilize compressible simulations, either alone or in the context of hybrid methods (i.e., in conjunction with non-dissipative schemes, with sensor-based switching). Examples include the HLLC [8] and WENO methods [9]. These schemes are generally thought to be unsuitable for turbulence due to the high levels of artificial dissipation introduced into the solution. The HLLC scheme is used as a prototype of a *dissipative* scheme for this work.

In the specific context of real-gas frameworks, a double-flux approach [18] was recently implemented by Ma et al. [16]. In this method, the internal energy is fixed within the time-integration step to artificially enforce pressure equilibrium, at the expenses of modifying the thermodynamics, thus recovering the following relation between internal energy and pressure

$$e = \frac{Pv}{\gamma^* - 1} + e_0^*, \tag{23}$$

where e_0^* and γ^* are in this case nonlinear functions of the thermodynamic states. Therefore, these two variables are frozen both in space and time during each time step.

Table 1 summarizes the numerical methods analyzed and tested in this work.

4 NUMERICAL RESULTS

4.1 Taylor-Green Vortex (ideal-gas thermodynamics)

A 3D inviscid Taylor-Green Vortex (TGV) [26] test is preliminary conducted to assess the energy-conservation properties of some of the approaches introduced in Section 1. Simulations are conducted in a periodic cube of size 2π with 32^3 grid points, CFL = 0.3 and a fourth-order Runge-Kutta scheme, using an ideal-gas thermodynamic model. Figure 2 clearly highlights the advantage of employing the KGP scheme, which strongly preserves kinetic-energy throughout an entire flow turn-over time, whereas the divergence approach leads to blow-up; although filtering techniques and upwind scheme (HLLC) are also stable, the dissipation is significant and therefore these schemes are unsuitable for studying supercritical high-pressure turbulence.

4.2 1D advection test (real-gas thermodynamics)

The 1D advection test proposed in [16] is carried out to assess the behaviour of numerical methods in a real-gas framework, particularly in terms of pressure oscillations. The test is

Numerical scheme	Description	References
Divergence	Conservative discretization of convection $C = \frac{\partial \rho u_j \phi}{\partial x_j}$	[12] Eq. (8)
Divergence + filter	Gaussian filter (conservative variables) $\bar{\phi} = \phi + \frac{\bar{\triangle}^2}{24}\frac{\partial^2 \phi}{\partial x_i^2} + \mathcal{O}\bar{\triangle}^4$	[6] Eq. (22)
HLLC	Upwind-biased shock-capturing scheme	[8]
KGP	Kinetic-energy preserving (KEP) $C = 1/4C^D + 1/4C^\phi + 1/4C^u + 1/4C^\rho$	[10, 11, 12] Eq. (14)
Shima et al.	Pressure-equilibrium preserving (PEP) $\widetilde{\mathcal{I}}\|_{(m\pm1/2)} = \frac{\rho e\|_{(m\pm1)} + \rho e\|_{(m)}}{2}\frac{u_j\|_{(m\pm1)} + u_j\|_{(m)}}{2}$	[14] Eq. (21)
Double-flux w/HLLC	Frozen thermodynamics $e = \frac{Pv}{\gamma^* - 1} + e_0^*$	[16] Eq. (23)
Double-flux w/KGP	e_0^* and γ^* nonlinear functions	

Table 1: Summary of numerical methods considered in this work.

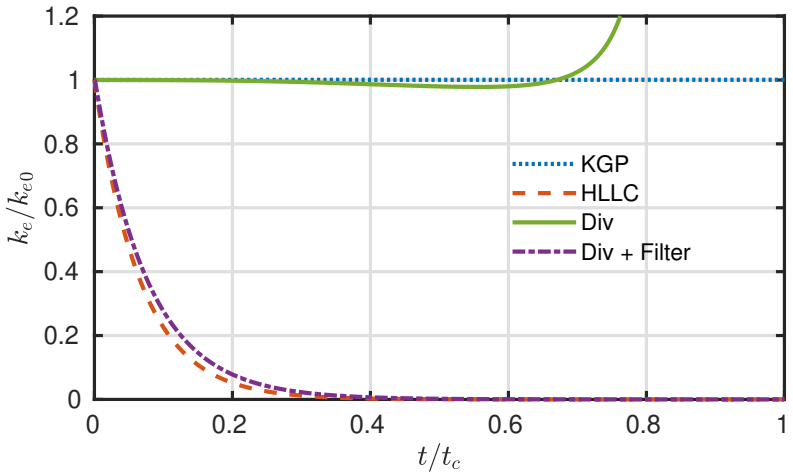

Figure 2: Results for inviscid 3D TGV [26]. Normalized kinetic energy for KGP (dotted blue line), HLLC (dashed red line), divergence method (solid green line) and divergence with filtering (dashed-dotted purple line) across normalized turn-over time t_c corresponding to $\sim L/u = 2\pi$ s.

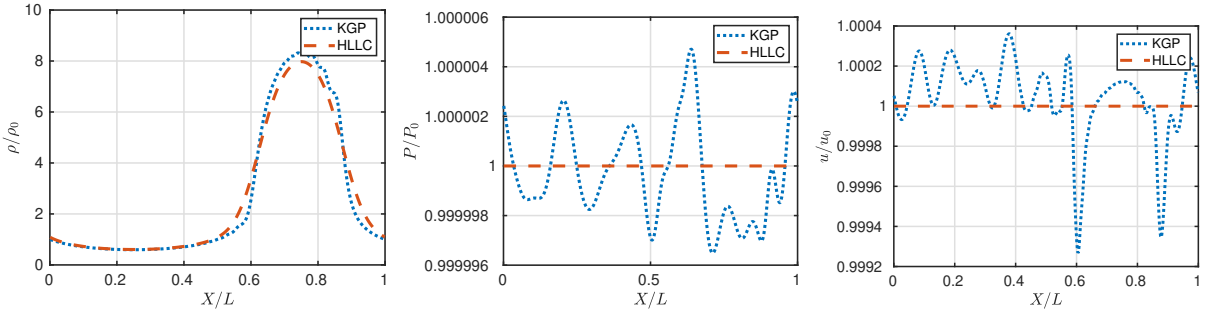

(a) (b) (c)

Figure 3: 1D Advection test [16] under a real-gas framework in a domain of length $L = 1$. N_2 is considered at $P_0 = 5\,\text{MPa}$, $u_0 = 1\,\text{m/s}$, smooth temperature profile given the harmonic wave $T = \frac{T_{min}+T_{max}}{2} + \frac{T_{max}-T_{min}}{2}\sin(2\pi\, x)$ with $T_{min} = 100\,\text{K}$ and $T_{max} = 300\,\text{K}$ and reference density $\rho_0 = 95.496\,\text{kg/m}^3$ (corresponding to $T = 200\,\text{K}$). Results shown after 1 s for KGP (dotted line) and HLLC (dashed line) convective schemes in conjunction with double-flux method for thermodynamics: normalized (a) density, (b) pressure and (c) velocity.

performed with a domain length of $L = 1\,\text{m}$, 512 grid points and CFL = 1. The double-flux approach outlined in Section 3.3 is employed in conjunction with both the HLLC scheme and the KGP method. The results reported in Figure 3 show that the double-flux technique is unable to suppress pressure oscillations when coupled with the KGP, while it achieves pressure equilibrium when used with the dissipative HLLC. While KEP and PEP schemes are able to preserve kinetic energy by convection irrespective of the thermodynamic model, they are unable to prevent pressure oscillations in a real-gas framework, whether they are used in conjunction with the double-flux model or not (results not shown here).

4.3 Assessment summary

Table 2 summarizes the properties satisfied in either ideal or real-gas frameworks for the schemes presented within this work. Therefore, the enforcement of pressure equilibrium while preserving kinetic energy needs further work, and future directions are outlined in Section 5.

5 SUMMARY, CONCLUSIONS & FUTURE WORK

This exploratory work has focused on identifying the discrete properties needed to accurately simulate high-pressure supercritical fluids turbulence, and assessing the performance of numerical schemes available in the literature in this regard. The properties identified mainly correspond to: (i) stability against spurious pressure oscillations resulting from the inherent non-linearities of real-gas thermodynamics, and (ii) low dissipation and conservation of kinetic energy to properly capture the broadband nature of turbulence. In particular, several state-of-the-art numerical schemes have been assessed in a 1D inviscid advection test at constant pressure and velocity to verify the discrete pressure equilibrium behaviour, and in a 3D inviscid TGV problem to analyze the discrete conservation properties.

The results obtained allow to conclude that the KGP scheme is able to preserve kinetic energy for ideal- and real-gas conditions. However, this scheme is not able to avoid spurious pressure

	KEP	PEP	Numerical stability	Low dissipation
Divergence	×	○	×	⊙
Divergence + filter	×	○	○	×
HLLC	×	○	⊙	×
KGP	⊙	×	○	⊙
Shima	⊙	○	○	⊙
Double-flux w/HLLC	×	⊙	⊙	×
Double-flux w/KGP	⊙	×	×	⊙

Table 2: Summary of numerical schemes assessment; ○ property applies only to ideal-gas, ⊙ property applies also to real-gas, × property is not satisfied in any framework.

oscillations for ideal gases, a fact that is intensified by the non-linearities present in real gases and resulting in blow-up of the solutions. The scheme proposed by Shima et al. [14] is also able to conserve kinetic energy at the discrete level and in addition, it avoids the appearance of artificial pressure oscillations in the case of ideal gases. Nonetheless, this scheme has been derived for ideal gases, and consequently does not suppress spurious pressure oscillations at high-pressure supercritical fluid conditions. On the other hand, strategies recently developed specifically for this problem, like for example the double-flux scheme, are able to mitigate pressure oscillations, but at the expenses of requiring artificial dissipation based on upwind-biased schemes and/or additional terms in the equations of mass and momentum conservation. As a result, to the authors' knowledge, there is currently no method able to simultaneously conserve kinetic energy and avoid artificial pressure oscillations for real-gas frameworks.

The preliminary results obtained in this work motivate the authors to (i) continue a careful assessment of numerical methods for high-pressure supercritical fluids turbulence, and (ii) focus on the development of PEP & KEP schemes for real-gas frameworks.

ACKNOWLEDGEMENTS

This work is supported by the European Research Council (ERC) under the European Union's Horizon Europe research and innovation programme (grant agreement No. 101040379 - SCRAMBLE), the *Formació de Professorat Universitari* scholarship (FPU-UPC R.D 103/2019) of the Technical University of Catalonia - BarcelonaTech (Spain), the *Serra Húnter* programme (Catalonia), and the *Beatriz Galindo* programme (Distinguished Researcher, BGP18/00026) of the *Ministerio de Ciencia, Innovación y Universidades* (Spain).

References

[1] L. Jofre and J. Urzay. A characteristic length scale for density gradients in supercritical monocomponent flows near pseudoboiling. *Annual Research Briefs, Center for Turbulence Research, Stanford University*, pages 277–282, 2020.

[2] L. Jofre and J. Urzay. Transcritical diffuse-interface hydrodynamics of propellants in high-

pressure combustors of chemical propulsion systems. *Prog. Energy Combust. Sci.*, 82:100877, 2021.

[3] M. Bernades and L. Jofre. Thermophysical analysis of microconfined turbulent flow regimes at supercritical fluid conditions in heat transfer applications. *J. Heat Transfer*, 144:082501, 2022.

[4] K. R. Sreenivasan. Turbulent mixing: a perspective. *PNAS*, 116:18175–18183, 2019.

[5] M. R. Visbal and D. V. Gaitonde. On the use of higher-order finite-difference schemes on curvilinear and deforming meshes. *J. Comput. Phys.*, 181:155–185, 2002.

[6] P. Sagaut and R. Grohens. Discrete filters for large eddy simulation. *Int. J. Numer. Methods Fluids*, 31:1195–1220, 1999.

[7] J. Larsson, S.K. Lele, and P. Moin. Effect of numerical dissipation on the predicted spectra for compressible turbulence. *Annual Research Briefs, Center for Turbulence Research, Stanford University*, pages 47–52, 2007.

[8] F. Toro. *Riemann solvers and numerical methods for fluid dynamics*. Springer (USA), 3rd edition, 2009.

[9] C.W. Shu. High order ENO and WENO schemes for computational fluid dynamics. *Lecture Notes in Computational Science and Engineering*, 9:439–582, 1999.

[10] C. A. Kennedy and A. Gruber. Reduced aliasing formulations of the convective terms within the navier–stokes equations for a compressible fluid. *J. Comput. Phys.*, 227(3):1676–1700, 2008.

[11] S. Pirozzoli. Generalized conservative approximations of split convective derivative operators. *J. Comput. Phys.*, 229:7180–7190, 2010.

[12] G. Coppola, F. Capuano, S. Pirozzoli, and L. de Luca. Numerically stable formulations of convective terms for turbulent compressible flows. *J. Comput. Phys.*, 382:86–104, 2019.

[13] G. Coppola, F. Capuano, and L. de Luca. Discrete energy-conservation properties in the numerical simulation of the navier–stokes equations. *Appl. Mech. Rev.*, 71(1), 2019.

[14] N. Shima, Y. Kuya, Y. Tamaki, and S. Kawai. Preventing spurious pressure oscillations in split convective form discretization for compressible flows. *J. Comput. Phys.*, 427:110060, 2021.

[15] S. Kawai, H. Terashima, and H. Negishi. A robust and accurate numerical method for transcritical turbulent flows at supercritical pressure with an arbitrary equation of state. *J. Comput. Phys.*, 300:116–135, 2015.

[16] P. C. Ma, Y. Lv, and M. Ihme. An entropy-stable hybrid scheme for simulations of transcritical real-fluid flows. *J. Comput. Phys.*, 340:330–357, 2017.

[17] G. Lacaze, T. Schmitt, A. Ruiz, and J. Oefelein. Comparison of energy-,pressure- and enthalpy-based approaches for modeling supercritical flows. *Computers Fluids*, 181:35–56, 2019.

[18] R. Abgrall and S. Karni. Computations of compressible multifluids. *J. Comput. Phys.*, 169:594–623, 2000.

[19] H. Terashima and M. Koshi. Approach for simulating gas-liquid-like flows under supercritical pressures using a high-order central differencing scheme. *J. Comput. Phys.*, 231:6907–6923, 2012.

[20] D. Y. Peng and D. B. Robinson. A new two-constant equation of state. *Ind. Eng. Chem. Fundam.*, 15:59–64, 1976.

[21] W. C. Reynolds and P. Colonna. *Thermodynamics: Fundamentals and Engineering Applications*. Cambridge University Press, Cambridge (UK), 1st edition, 2019.

[22] A. Burcat and B. Ruscic. Third millennium ideal gas and condensed phase thermochemical database for combustion with updates from active thermochemical tables. Technical report, Argonne National Laboratory, 2005.

[23] F. Capuano, G. Coppola, L. Rández, and L. de Luca. Explicit Runge–Kutta schemes for incompressible flow with improved energy-conservation properties. *J. Comput. Phys.*, 328:86–94, 2017.

[24] A. Báez Vidal, O. Lehmkuhl, F. X. Trias, and C. D. Pérez-Segarra. On the properties of discrete spatial filters for CFD. *J. Comput. Phys.*, 326:474–498, 2016.

[25] F. Capuano, A. Mastellone, and E.M. De Angelis. A conservative overlap method for multi-block parallelization of compact finite-volume schemes. *Computers & Fluids*, 159:327–337, 2017.

[26] E. Johnsen, J. Larsson, A. V. Bhagatwala, W. H. Cabot, P. Moin, B. J. Olson, P. S. Rawat, S. K. Shankar, B. Sjögreen, H. C. Yee, Z. Zhong, and S. K. Lele. Assessment of high-resolution methods for numerical simulations of compressible turbulence with shock waves. *J. Comput. Phys.*, 229(4):1213–1237, 2010.